Published in final edited form as:
J Immunol. 2013 July 1; 191(1): 228–237. doi:10.4049/jimmunol.1202905.

Enhanced T Cell Function in a Mouse Model of Human Glycosylation

George Buchlis[*,†], **Pamela Odorizzi**[*], **Paula C. Soto**[‡], **Oliver M. T. Pearce**[‡], **Daniel J. Hui**[†], **Martha S. Jordan**[*], **Ajit Varki**[‡], **E. John Wherry**[*], and **Katherine A. High**[*,†,§]

[*]University of Pennsylvania School of Medicine, Philadelphia, PA, United States

[†]Pediatrics-Hematology, Children's Hospital of Philadelphia, Philadelphia, PA, United States

[‡]Medicine and Cellular and Molecular Medicine, University of California at San Diego, La Jolla, CA, United States

[§]Howard Hughes Medical Institute, Philadelphia, PA, United States

Abstract

Clinical evidence for a more active immune response in humans compared to our closest hominid relative, the chimpanzee, includes the progression of HIV infection to AIDS, Hepatitis B and C related inflammation, autoimmunity, and unwanted harmful immune responses to viral gene transfer vectors. Humans have a unique mutation of the enzyme cytidine monophosphate-N-acetylneuraminic acid hydroxylase (CMAH), causing loss of expression of the sialic acid Neu5Gc. This mutation, occurring 2 million years ago, likely altered the expression and function of ITIM-bearing inhibitory receptors (Siglecs) that bind sialic acids. Previous work showed that human T cells proliferate faster than chimpanzee T cells upon equivalent stimulation. Here we report that Cmah−/− mouse T cells proliferate faster and have greater expression of activation markers than wild-type mouse T cells. Metabolically re-introducing Neu5Gc diminishes the proliferation and activation of both human and murine Cmah−/− T cells. Importantly, Cmah−/− mice mount greater T cell responses to an Adenovirus encoding an Adeno-associated Virus capsid transgene (Ad-AAV). Upon Lymphocytic Choriomeningitis Virus (LCMV) infection, Cmah−/− mice make more LCMV-specific T cells than WT mice, and these T cells are more polyfunctional. Therefore a uniquely human glycosylation mutation, modeled in mice, leads to a more proliferative and active T cell population. These findings in a human-like mouse model have implications for understanding the hyper immune responses that characterize some human diseases.

INTRODUCTION

Mammalian cells are coated with a complex layer of glycans that mediate pathogen binding, cell adhesion, cell trafficking, cell signaling, endocytosis, apoptosis, and proliferation(1). Although heterogeneity in the expression and structure of these glycan chains can exist within the same individual and even within the same organ, an interesting species-specific divergence in these sugars was discovered in 1998. Two groups reported the human-specific inactivating mutation of the enzyme CMP-N-acetylneuraminic acid hydroxylase, or CMAH, which is responsible for the conversion of sialic acid precursor CMP-Neu5Ac to CMP-Neu5Gc by the addition of a single hydrogen atom(2, 3). As a result, Neu5Gc is not synthesized in human cells and is in fact immunogenic(4, 5). This mutation appears to have

Correspondence: Katherine A. High M.D. Room 5060, Colket Translational Research Building, 3501 Civic Center Blvd. Philadelphia, PA 19104, Phone: 215-590-4521, Fax: 215-590-3660, high@email.chop.edu.

set in motion a series of genetic and biochemical changes in the biology of sialic acids that may contribute to several unique aspects of human biology in health and disease(6, 7).

Of the many functions that sialic acids play in cellular physiology, their role as ligands of inhibitory Siglecs is well recognized. Siglecs, or sialic acid-binding immunoglobulin superfamily lectins, are broadly and variably expressed on cellular surfaces of the mammalian immune system and have unique binding preferences for the type of sialic acid and its linkage to the underlying glycan chain(8). Many Siglecs, including CD22 and most of the CD33-related Siglecs, contain immunoreceptor tyrosine-based inhibitory motifs (ITIMs) in their cytoplasmic tails, which when phosphorylated by Src family kinases, recruit phosphatases that attenuate downstream signaling(9, 10). A number of studies have characterized the inhibitory effects of Siglecs in human(11–15) and murine(16–18) immune systems. Humans lost expression of Siglec-5 on T cells, which potentially occurred as a result of genetic pressure on Siglec loci after the loss of CMAH function and thus the absence of sialic acid ligand Neu5Gc. Subsequent investigation showed that when equivalently stimulated, human T cells proliferate much faster than non-human primate T cells, and this proliferation can be slowed by expressing Siglec-5 in the human T cells(19, 20).

Interestingly, humans are much more prone to AIDS progression during HIV infection when compared to HIV-infected chimpanzees and West African chimpanzees that are hosts for related simian immunodeficiency viruses. One hypothesis for human progression to AIDS is that enhanced activation of the human immune system in response to HIV eventually leads to exhaustion and death of CD4+ T cells(7). The hepatitis viruses provide another example of differences in immune response; a large proportion of humans infected with Hepatitis B (HBV) or Hepatitis C (HCV) virus progress to chronic active hepatitis, while the disease tends to be acute and self-limited in chimpanzees. Even in those unusual cases that progress to chronic infection in HBV and HCV-infected chimpanzees, the severity of complications related to these pathologies is reduced compared to humans. Many of the late complications of hepatitis in humans are due to an overactive immune response, and not the cytopathic effect of the virus itself(7). Finally, in recent clinical trials with viral vectors, humans mounted T cell immune responses to Adeno-associated viral (AAV)-mediated gene transfer that were unanticipated from preclinical animal studies, even in non-human primates that are natural hosts for AAV(21, 22). Attempts by a number of groups at recapitulating these results in mice have been uniformly unsuccessful(21, 23–26). Thus a human-specific glycosylation mutation that potentially disrupts ITIM-mediated immune suppression is of interest in analyzing humans' unique susceptibility to these immune response-related pathologies.

Recently, a Cmah−/− mouse has been generated to assess the effect of this human enzyme mutation in the context of both normal and disease settings in an animal model(27, 28). Initial studies in these mice showed human-like features such as delayed wound healing and age related hearing loss, and a human-like muscular dystrophy phenotype following combined mutation of the dystrophin gene(29). Immunologically these mice seem to have enhanced B cell proliferation and antibody production, which is consistent with the observation that Neu5Gc is physiologically down-regulated during normal B cell activation(28). In addition, a recent publication showed a similar down-regulation of CMAH function and Neu5Gc levels in activated wild-type murine T cells(30).

We hypothesized that mice engineered to mimic the human mutation of the Cmah gene would display enhanced T cell responses to in vitro and in vivo stimulation. We found that, upon equivalent T cell stimulation in vitro, Cmah−/− T cells proliferated faster, had greater expression of activation markers, and secreted more IFNγ than wild-type (WT) T cells.

Additionally, the responses in both human T cells (which are naturally Cmah-deficient) and Cmah−/− mouse T cells were blunted by reintroducing the missing Neu5Gc sialic acid onto the cell surface via metabolic incorporation from the culture media. Immunization of Cmah −/− mice with an Adenoviral vector encoding the AAV capsid elicited a stronger T cell response in Cmah−/− mice compared to wild-type littermate mice. Finally, we asked whether the robust T cell immune responses of Cmah−/− mice were seen in the context of a live replicating viral infection. Cmah−/− mice infected with acute Lymphocytic Choriomeningitis Virus (LCMV) strain Armstrong developed more LCMV specific T cells in the blood and spleen. Importantly, LCMV peptide-stimulated splenic T cells from Cmah −/− mice produced a higher proportion of cytokines than WT T cells at day 42 post-infection. These findings shed light on the role that glycosylation plays in immune regulation, and may give evolutionary insight into the etiology of overactive immune pathologies in humans.

MATERIALS AND METHODS

Mice

Cmah−/− mice generated as described(27) and back-crossed to C57BL/6 mice more than 10 generations were bred with C57BL/6 mice purchased from Jackson Labs to obtain heterozygous breeding pairs. Heterozygous breeding pairs were then mated, creating Cmah −/−, Cmah+/−, and Cmah+/+(essentially WT and will be referred to as such in this manuscript) mice. The Cmah−/− and WT mice were used in experiments as littermates, and surplus Cmah+/− heterozygous mice were saved for future mating. Mice were bred and maintained, and investigations conducted, according to an approved Children's Hospital of Philadelphia Institutional Animal Care and Use Committee protocol.

In Vitro Proliferation and Activation Assays

Naïve Cmah−/− and WT mouse spleens were harvested, and splenocytes were isolated using a 70μm nylon cell strainer and plunger. Isolated splenocytes were either directly labeled with Cell Trace CFSE (Invitrogen) and plated in culture, or subjected to $CD8^+$ T cell isolation using the $CD8^+$ T Cell Negative Isolation Kit (Dynal/Invitrogen) and then labeled with CFSE. 2E6 CFSE labeled cells were plated with 25μL α-CD3/α-CD28 activator beads (Dynal/Invitrogen) in 1mL AIM V culture medium (GIBCO) supplemented with 3% FBS, Penicillin/Streptomycin, and Glucose. Cells were cultured in these conditions for 3 or 5 days, harvested, washed, and stained with 1:100 α-CD62L-PE (BD Bioscience) and 1:100 α-CD25-APCCy7 (BD Bioscience) for 30 minutes at 4 degrees Celsius. Cells were washed twice and resuspended in 4% Paraformaldehyde solution and read on a FACS CantoII (BD) flow cytometer.

Neu5Gc Feeding Experiments

Mouse T cell experiments—5μM CFSE-labeled negatively isolated mouse T cells were cultured for 2 days in 6mM Neu5Gc- or Neu5Ac containing media, stimulated with immobilized α-CD3 (200ng/mL) and soluble α-CD28 (1μg/mL), and analyzed for CD69 (α-CD69-PE, BD) expression and CFSE dilution after 5 days.

Human T cell experiments—Isolated human CD4 T cells were cultured for 3 days in 3mM Neu5Gc- or Neu5Ac containing media, stimulated with immobilized α-CD3 (25ng/mL) and soluble α-CD28 (1μg/mL), and analyzed for CD25 expression after 2 days. For proliferation analysis, human PBMC were labeled with 5μM CFSE, stimulated with immobilized α-CD3 (25ng/mL) and soluble α-CD28 (1μg/mL) for 5 days, and analyzed for CFSE dilution. Neu5Gc and Neu5Ac sialic acid stocks were synthesized as described(31).

In Vitro Stimulation

Isolated splenocytes were plated at either 1E6/200μL (LCMV and AAV peptide stimulations) or 1E6/500μL (PMA and α-CD3 stimulations) and incubated for 5 hours in either 10% FBS RPMI (GIBCO, LCMV stimulations) or 3% FBS AIMV media as described above (AAV peptide, PMA, and α-CD3 stimulations). For PMA, α-CD3, and AAV peptide stimulations, 1μL of BD GolgiStop (BD) was added to the stimulation medium to block transport and intracellularly accumulate cytokines. For LCMV stimulations, 1:500 GolgiStop and 1:1000 GolgiPlug (BD) were added to the stimulation media, along with 1:1000 α-CD107a-Alexa Fluor 488 (Biolegend). Stimulant concentrations were as follows: PMA-50ng/mL along with 1μg/mL ionomycin, α-CD3-1μg/mL, AAV2 H2Kb peptide (SNYNKSVNV)-5μg/mL(32), LCMV GP276 or GP66-77 peptides-0.4ng/mL.

Intracellular Cytokine Staining

Surface Stains—After 5 hours of stimulation, cells were harvested, washed, and surface stained for 30 minutes at 4 degrees Celsius. LCMV stimulations: cells were stained for 20 minutes at room temperature with 1:600 Live/Dead Fixable Aqua Dead Cell Stain, washed, stained 30 minutes at 4 degrees Celsius with 1:400 α-CD4-PE Texas Red (Invitrogen) or 1:100 α-CD8-PE Texas Red (Invitrogen) and α-CD44-Alexa Fluor 700 (Biolegend). AAV stimulation: cells were stained for 30 minutes at 4 degrees Celsius with 1:100 α-CD8-Pacific Blue (Biolegend), and 1:100 α-CD44-APCCy7 (BD). PMA and α-CD3 stimulations: cells were stained for 30 minutes at 4 degrees Celsius with 1:100 α-CD8-FITC (BD) and α-CD4-PE (BD).

Intracellular Stains—Cells were washed twice, fixed and permeabilized with Cytofix/Cytoperm solution (BD) for 20 minutes at 4 degrees Celsius. Cells were washed twice with Perm Buffer (BD), and stained for 30 minutes at 4 degrees Celsius. LCMV stimulations: 1:100 α-IFNγ-PerCp-Cy5.5 (Biolegend), 1:100 α-TNFα-Pacific Blue (Biolegend), 1:20 α-Mip1α-PE (R&D Systems), and 1:100 α-IL-2-APC (eBioscience). AAV peptide, PMA, and α-CD3 stimulations: 1:100 α-IFNγ-APC (BD). Cells were washed twice with Perm Buffer, resuspended in fixative and read on either an LSRII (BD) or FACS CantoII.

Viral Infections

4 month old littermate WT and Cmah−/− mice were injected with either 50μL/leg intramuscularly in the quadriceps with 1E9 pfu/mouse (Ad-AAV experiments: Adenoviral human 5 construct encoding the AAV2 capsid proteins as a transgene(32)) or 300μL intraperitoneally with 2E5 pfu/mouse (LCMV experiments: Lymphocytic Choriomeningitis Virus Strain Armstrong). Mice were bled and sacrificed at day 10 post immunization (Ad-AAV immunization) or bled weekly until sacrifice at day 42 (LCMV infections). Blood was collected retroorbitally at various time points via heparinized microcapillary tubes (Fisher Scientific) into 1mL of 4% Sodium Citrate and 1mL 1% RPMI. Spleens were harvested and processed at sacrifice as previously described. Cells were washed, and then stained for surface markers.

Longitudinal Surface Stains and LCMV Plaque Assays

LCMV Experiment Stains—Stained first for 20 minutes at room temperature with 1:600 Live/Dead Fixable Aqua Dead Cell Stain, washed, then stained 30 minutes at 4 degrees Celsius with 1:100 α-KLRG1-FITC (Beckman Coulter), α-CD4-PE Texas Red (Invitrogen), α-CD8-Pacific Blue (Biolegend), α-CD127-PE (Biolegend), α-CD44-Alexa Fluor 700 (Biolegend), and LCMVGp33 Tetramer-APC.

AAV Experiment Stains—Stained 30 minutes at 4 degrees Celsius with 1:10 AAV-SNYNKSVNV Pentamer (Proimmune), 1:100 α-CD8-Pacific Blue (Biolegend), and 1:100 α-CD44-APCCy7 (BD). Cells were then washed twice, resuspended in fixative, and read on either an LSRII or FACS CantoII.

LCMV Plaque Assays—Spleen homogenates were titered for viral load using a Vero cell plaque assay as previously described(33).

Ly5.2 Donor CD8 Transfer into Ly5.1 Recipient Mice

Spleens were harvested from both Cmah−/− and WT mice and processed as previously described to obtain splenocytes. CD8 T cells were negatively isolated from mouse strain pooled splenocyte populations using the Dynal CD8 negative isolation kit. Since Cmah−/− mice are on a C57BL/6 WT background, they express the Ly5.2 isoform of CD45. We are thus able to transfer these cells into congenic recipient mice expressing Ly5.1 to track donor cells. 4–6 week old female Ly5.1 mice were purchased from either the NCI or Jackson labs to be used as recipient mice. 20E6 Ly5.2 naïve donor (Cmah−/− or WT) CD8 T cells were suspended in 200 μL RPMI and injected intravenously into the tail vain of recipient mice. Recipient mice were also infected with LCMV. Mice were bled and sacrificed at day 6–7, and PBMC and spleens were collected. Splenocytes and PBMC were stained with the standard panel described in the longitudinal surface stain methods.

Gating Strategy for Flow Cytometric Analysis

General gating schemes for the live viral infection analyses throughout the manuscript are described in Supplemental Figure 1. Briefly, cells were plotted forward scatter area vs. side scatter area to determine the lymphocyte population. After gating on the lymphocyte population, gates were subsequently made to only include singlets, and further gated on live cells. Then CD8+ cells were selected and either plotted for tetramer response or for cytokine analysis and IFNγ production.

Statistical Analysis

All statistical analysis was performed in GraphPad Prism software, and data significance was determined by 2-tailed student's t test.

RESULTS

In vitro T cell proliferation and activation is augmented in Cmah−/− mice

In order to assess T cell proliferation and activation in vitro, we isolated both Cmah−/− and WT splenocytes from naïve mice. We labeled total splenocytes with CFSE and plated them with α-CD3/α-CD28 activator beads for 5 days. By day 5, Cmah−/− CD8 T cells within the splenocyte population proliferated faster than their WT counterparts (Figure 1A), as did CD4 T cells (Supplemental Figure 2A). In addition to the observed enhanced dilution of CFSE, division and proliferation indices at 5 days were significantly greater in Cmah−/− CD8 T cells when compared to WT CD8 T cells (Figure 1B). Unstimulated splenocytes showed no difference in CFSE dilution after 5 days (Supplemental Figure 2C). This apparent difference in proliferation was not due to potential survival effects of the *Cmah* mutation, as both WT and Cmah−/− cultures had similar levels of cell death when compared to the expected number of cells at 5 days (Supplemental Figure 2F). Additionally, both Cmah−/− CD8 and CD4 T cells had lower levels of CD62L (L-selectin) than WT T cells, the loss of which is a hallmark of T cell activation (Figure 1A and 1B). Baseline levels of unstimulated CD8 and CD4 T cells showed no difference in CD62L levels (Supplemental Figure 2D and data not shown). To determine whether the heightened activation and

increased proliferation in Cmah−/− T cells was an intrinsic cell phenomenon, or was dependent on the context of other splenic populations, we negatively isolated CD8 T cells from naïve spleens of both Cmah−/− and WT mice. These CD8 T cells were CFSE labeled, plated at equal numbers, and activated for either 3 or 5 days with α-CD3/α-CD28 activator beads. Cmah−/− CD8 T cells had lower levels of CD62L and higher expression of IL-2Rα (CD25), which is upregulated during T cell activation. These differences emerged as early as day 3 post-stimulation and were sustained through day 5 (Figure 1C). Although there was a subtle increase in Cmah−/− CD8 T cell proliferation at day 3, they had proliferated to a much greater extent than WT CD8 T cells by day 5 (Figure 1C). To investigate whether the enhanced activation and proliferation observed in Cmah−/− versus WT CD8 T cells are associated with early signaling/activation differences, we evaluated CD62L and CD25 expression at early time points following TCR and CD28 stimulation. As early as 5 hours post-activation, there were significantly higher frequencies of Cmah−/− T cells that lost CD62L expression when compared to WT littermate CD8 T cells (Figure 1D). In addition, Cmah−/− CD8 T cells had higher levels of CD25 expression on their surface at 5 hours (Figure 1D). To assess if these differences in proliferation and activation markers corresponded to functional differences, we stimulated naïve T cells with Phorbol myristate acetate (PMA) and stained intracellularly for IFNγ production. After 5 hours of stimulation, a significantly higher frequency of Cmah−/− CD8 and CD4 T cells produced IFNγ when compared to WT T cells (Figure 1E). Similarly, Cmah−/− CD8 T cells stimulated for 5 hours with an α-CD3 antibody displayed a higher frequency of IFNγ-producing T cells when compared to WT CD8 T cells (Supplemental Figure 2B). Thus, Cmah−/− T cells more rapidly acquire an activated phenotype, proliferate faster, and produce more IFNγ than WT T cells upon equivalent T cell stimulation in vitro.

Metabolically re-introducing Neu5Gc to Cmah−/− T cells and human T cells blunts proliferation and activation

Since both human T cells and Cmah−/− T cells lack the ability to produce Neu5Gc sialic acid, we hypothesized that metabolically re-introducing Neu5Gc into these cells(34) via the culture media would blunt the previously observed enhanced activation and proliferation. We activated CFSE-labeled human PBMC and Cmah−/− mouse T cells for 5 days with immobilized α-CD3 and soluble α-CD28 in either Neu5Gc-containing media or Neu5Ac-containing control media. Efficient incorporation of Neu5Gc from the culture medium was visualized in human cells with an antibody recognizing Neu5Gc (Supplemental Figure 2E). Both human and Cmah−/− T cell proliferation was blunted by the introduction of the missing Neu5Gc sialic acid when compared to control Neu5Ac fed T cells, as seen by decreased dilution of CFSE at 5 days post activation (Figure 2A). When we pre-incubated human CD4 T cells for 3 days in Neu5Gc containing media and activated them for 2 days, they showed an approximately 50% reduction in CD25 expression over Neu5Ac control fed T cells, indicating that Neu5Gc feeding of human T cells blunts activation (Figure 2B). Similarly, pre-incubating Cmah−/− T cells for 2 days with Neu5Gc and activating them for 5 days greatly decreased activation marker CD69 levels in both CD4 and CD8 T cells when compared to Neu5Ac fed control T cells (Figure 2B). These results indicate that the metabolic re-introduction of missing sialic acid Neu5Gc to both human and Cmah−/− T cells blunts their activation and proliferation during in vitro stimulation.

Cmah−/− mice mount a greater CD8 T cell response to AAV after Ad-AAV immunization

We hypothesized that the absence of CMAH in humans may have contributed to the unanticipated immune responses seen in AAV gene therapy trials(21–23). To test this, we moved to an in vivo viral immune challenge, to correlate the in vitro hyperactivation of Cmah−/− T cells to an in vivo phenotype. We intramuscularly immunized Cmah−/− and WT mice with a human Adenovirus serotype 5 vector encoding the Adeno-associated Virus

serotype 2 capsid. No difference in AAV2-specific T cells was observed at baseline as expected (Figure 3A), and no difference in naïve T cell numbers was observed in the spleen of unimmunized mice (data not shown). However a significantly higher number of T cells against the AAV2 capsid were found in the peripheral blood of Cmah−/− mice at day 10 when compared to WT mice (Figure 3A). Though not as dramatic, an increase in Cmah−/− AAV2 capsid specific T cells over WT T cells was also seen in day 10 splenocytes (Figure 3B). Additionally, when we stimulated day 10 splenocytes with the H-2K^b AAV2 peptide SNYNKSVNV, we observed a significantly higher frequency of Cmah−/− T cells producing IFNγ when compared to WT T cells (Figure 3C). Therefore intramuscular immunization with Adenovirus expressing AAV2 capsid leads to a more robust CD8 T cell response at day 10 in Cmah−/− mice vs. WT mice.

Cmah−/− mice mount a greater T cell response during acute LCMV Armstrong infection

While the Adenovirus immunization results showed an enhanced T cell response in Cmah−/− mice, we sought to assess the T cell kinetics and activation during a live, replicating viral infection, predicting that Cmah−/− mice would mount a stronger T cell response during infection. To do this we infected Cmah−/− mice and WT mice with the acute Armstrong strain of Lymphocytic Choriomeningitis Virus (LCMV). Mice were bled longitudinally for PBMC analysis and sacrificed at day 42 for terminal splenocyte analysis. A representative flow cytometric gating strategy depicts how the data were analyzed (Supplemental Figure 1). At the peak of the T cell response on day 8 post-infection, we observed a dramatic increase in the frequency of total CD8 T cells in the blood of Cmah−/− mice when compared to WT mice (Figure 4A). We also observed significantly more Cmah−/− T cells directed against the gp33 epitope of LCMV at day 8 in the blood, and this difference remained significant throughout the duration of the 42-day study (Figure 4B). Furthermore, we saw a marked increase in the number of LCMV-specific KLRG1-CD127+ memory precursor T cells in Cmah−/− mice vs. WT mice. This difference was apparent at day 14 post-infection and remained significant in the blood at day 42 (Figure 4C). Interestingly, there was no difference in splenic LCMV viral titers during the course of the infection between Cmah−/− and WT mice (Supplemental Figure 4). At day 42 post-infection, Cmah−/− mice also had a higher frequency of LCMV-specific CD8 T cells in the spleen compared to WT mice (Figure 4D), and a higher frequency of these LCMV-specific T cells were memory precursor KLRG1-CD127+ (Figure 4E). In an attempt to determine if the in vivo response to LCMV is CD8 autonomous, we transferred 20E6 CD8 T cells from either Cmah−/− or WT mice into congenic Ly5.1 mice. Since Cmah−/− and WT littermates are on a C57BL/6 background, they are Ly5.2 positive and can be tracked in the Ly5.1 recipient mice. Recipient mice were infected with LCMV and sacrificed at day 6–7 to analyze PBMC and splenocytes. We observed greater numbers of Cmah−/− gp33+ donor CD8's in the spleen and a trend for greater numbers in the PBMC when compared to the response of WT CD8 T cells in recipient mice (Figure 4F). This supports the hypothesis that the observed CD8 T cell response to LCMV infection is CD8 autonomous. Thus, after a live viral infection with LCMV, Cmah−/− mice generate a greater number of LCMV-specific T cells in the blood and spleen compared to wild type mice. Additionally, a greater proportion of the Cmah−/− LCMV-specific T cell compartment is composed of KLRG1-CD127+ memory precursor cells.

LCMV-specific T cells in Cmah−/− mice produce a higher proportion of cytokines than WT T cells

We also hypothesized that T cells generated against LCMV were themselves more functional in Cmah−/− mice vs. WT mice. To test this, we stimulated equal numbers of day 42 splenocytes from Cmah−/− and WT mice with LCMV peptides and stained for intracellular cytokine production. We observed a higher proportion of IFNγ+ Mip1α+ T

cells in Cmah−/− mice compared to WT mice (Figure 5A and 5B), which correlated well with the observed increase in LCMV-specific T cells by tetramer staining. To assess the polyfunctionality of the CD8 T cell compartment, we looked at production of TNFα and IL-2 by the IFNγ+ Mip1α+ T cells. A significantly greater proportion of Cmah−/− Mip1α +IFNγ+ CD8 T cells made both TNFα and IL-2 when compared to WT CD8 T cells (Figure 5C). Similar trends in increased T cell functionality were observed in day 8 splenocytes (Supplemental Figure 3). Furthermore, Cmah−/− mice had an increase in the proportion of day 42 CD8 T cells capable of performing multiple functions simultaneously (expression of CD107a, Mip1α, IFNγ, TNFα, and IL-2) upon peptide stimulation. This was especially evident in the fraction of CD8 T cells that produced 4 or 5 functions simultaneously (Figure 5D and 5E). In sum, the T cell response to LCMV Armstrong in Cmah−/− mice is more robust than the response seen in WT mice.

DISCUSSION

Several theories have been proposed to explain the loss of function of the CMAH enzyme in humans after their evolutionary divergence from non-human hominids. One holds that a pathogen that bound Neu5Gc sialic acid may have been so detrimental to human survival that the mutation of CMAH and thus the loss of Neu5Gc expression allowed humans to escape this pathogen(7, 35). This would have placed an enormous benefit on fixing this mutation in the human population, perhaps even at the cost of reduced interaction of glycans with ITIM-bearing inhibitory receptors and altered immunological effects.

In our study, we showed that Cmah−/− mouse T cells had higher levels of activation markers and proliferated faster in vitro upon equivalent stimulation when compared to WT mice. These results are similar to studies done in human vs. chimpanzee T cells, where human T cells proliferate more than equivalently stimulated chimpanzee T cells(19, 20). In those human vs. chimpanzee studies, it was hypothesized that the loss of Siglecs on human T cells, likely a result of evolution from the loss of CMAH function, reduced the inhibitory threshold for activation. Accordingly, Siglec-5 transfection of human T cells was able to blunt the proliferation effect. In our study, we metabolically reintroduced Neu5Gc sialic acid via the culture media of both human and Cmah−/− T cells and observed reduced proliferation and activation.

The observed blunting of proliferation and activation upon Neu5Gc feeding fits well with a recent study that reported a physiological reduction of CMAH function and Neu5Gc expression during normal murine T cell activation(30). This paper showed decreased binding of activated T cells to several ITIM-bearing Siglecs, including CD22, a known B cell inhibitory Siglec that preferentially binds Neu5Gc. Less clear is the presence of these Siglecs on murine T cells, with the exception of one study which showed CD22 on some murine T cells(36). Indeed we confirmed that CD22 is both transcribed and expressed on WT and Cmah−/− T cells, albeit on a subset of the total population (data not shown). Therefore the loss of Neu5Gc may have rendered these cells more readily activated, since there would be less CD22 (and thus less associated phosphatase activity) clustering with sialylated receptors at the surface. While this may be a suitable explanation for the subset of cells expressing CD22, we cannot conclude that this is entirely responsible for the observed proliferation and activation differences. Future studies should focus on additional identification of Siglecs on murine T cells, whether there are membrane steric or electric charge effects due to the additional oxygen atom in Neu5Gc sialic acid, and if there are differences in the turnover of these sialic acids on the cell surface under varying physiological conditions.

When we challenged mice in vivo with a live, replicating acute strain of LCMV (Armstrong), Cmah−/− mice generated greater numbers of CD8 T cells directed against the LCMV virus. The higher frequencies of LCMV-specific T cells are likely a result of reduced activation thresholds and corroborate the observed increases in proliferation and activation in vitro. Previous studies have shown that a long lived memory T cell population arises from a killer cell lectin-like receptor G1 (KLRG1) low, IL-7Rα (CD127) high subset of antigen specific cells(37, 38). Interestingly, among the LCMV-specific T cells, there was a higher frequency of KLRG1-CD127+ memory-precursor T cells in Cmah−/− mice. This precursor difference did not seem to be due to a difference in LCMV viral load kinetics in the spleen at days 3, 5, and 7 (Supplemental Figure 4). It remains possible that even a minor change in antigen level that we may not have detected could have led to differences in memory formation, as antigen removal is known to lead to memory transition of T cells(39). Other factors known to influence memory T cell formation include CD4 T cell help(40), the strength and duration of TCR stimulation(39, 41, 42), inflammation during T cell activation(39, 41), and clonal competition(42). While we observed enhanced CD4 responses in Cmah−/− mice, it is unclear whether this affected the quantity of memory precursor cells. We additionally observed qualitatively enhanced CD8 responses at day 42 in Cmah−/− null mouse splenocytes. These CD8 cells were highly polyfunctional upon LCMV peptide stimulation, simultaneously degranulating and producing high levels of IFNγ, TNFα, and IL-2, a hallmark of memory T cells. We therefore conclude that Cmah−/− mice make a more functional response upon LCMV antigen stimulation at a memory time point when compared to WT littermate mice.

We also showed that Cmah−/− mice immunized with an Adenovirus vector encoding the Adeno-associated virus capsid (Ad-AAV) mounted a greater T cell response to the AAV capsid transgene when compared to WT mice. This finding is of particular relevance to recent clinical results in trials of AAV-mediated gene transfer of Factor IX to the liver of men with severe hemophilia B. Animal gene transfer models had failed to predict a T cell-mediated immune response directed against the AAV capsid that resulted in transient elevation in liver enzymes and a loss of the donated gene in patients with severe hemophilia(21, 22). Subsequent attempts to develop an animal model that accurately mimicked the observed T cell responses in humans were unsuccessful(24–26, 43). The generally accepted hypothesis accounting for immune responses generated against the AAV vector in humans is that a pre-existing memory pool of T cells from an early childhood infection is reactivated upon gene transfer and attacks virally-infected cells(44). While it is certainly the case that most pre-clinical animal studies were performed in naïve hosts, non-human primates (NHP) are also natural hosts for AAV. It has been shown that in spite of the presence of CD8 T cells specific for AAV in NHP, humans have a more polyfunctional resident memory population of AAV specific T cells, whereas NHP have a population of CD8 T cells with an effector cell phenotype that seems to be less functional upon stimulation(45). In preclinical gene transfer studies in which NHP were infused with AAV, there was no observed T cell response or transaminitis(46–48).

To put our results in a wider context, there are many instances of what might be termed inappropriate immune responses in human pathology, including autoimmune disease, chronic inflammation, and the progression of HIV infection to AIDS. These pathologic conditions are not as frequent in other species and, for research purposes, are generally experimentally induced, since they are not naturally occurring. Many changes over human evolution have likely contributed to the presently heightened immune response in humans compared to other species. However our findings of augmented T cell responses, in a mouse with a uniquely human glycosylation mutation likely to alter binding to ITIM-bearing inhibitory receptors, highlight the relationship between glycosylation and immune regulation in human pathology.

Supplementary Material

Refer to Web version on PubMed Central for supplementary material.

Acknowledgments

This work was supported by the National Institutes of Health (P01 HL078810 to K.A.H., P01 HL107150 to A.V., and T32-HL07439 to G.B.) and the Howard Hughes Medical Institute

G.B. wrote the manuscript. G.B., P.M.O., P.C.S., A.V., E.J.W., and K.A.H. designed experiments. G.B., P.M.O., P.C.S., O.M.T.P, M.S.J., A.V., E.J.W., and K.A.H. edited the manuscript. O.M.T.P. synthesized Neu5Gc and Neu5Ac sialic acids. M.S.J. assisted with signaling analysis. D.J.H. assisted in sample processing. G.B., P.M.O., and P.C.S. performed and analyzed experiments. The authors would like to acknowledge Robert Davidson for assistance with animal procedures, and Dr. Sarah Ratcliffe for helpful discussion on statistical analysis. They additionally acknowledge Drs. Robert H. Vonderheide, Michael R. Betts, Kyong-Mi Chang, and all members of the High, Wherry, Koretzky, and Varki labs for helpful comments and discussion.

References

1. Varki A, Lowe JB. Biological Roles of Glycans. Essentials of Glycobiology. 2009
2. Chou HH, Takematsu H, Diaz S, Iber J, Nickerson E, Wright KL, Muchmore EA, Nelson DL, Warren ST, Varki A. A mutation in human CMP-sialic acid hydroxylase occurred after the Homo-Pan divergence. Proc Natl Acad Sci USA. 1998; 95:11751–11756. [PubMed: 9751737]
3. Irie A, Koyama S, Kozutsumi Y, Kawasaki T, Suzuki A. The molecular basis for the absence of N-glycolylneuraminic acid in humans. J Biol Chem. 1998; 273:15866–15871. [PubMed: 9624188]
4. Brinkman-Van der Linden EC, Sjoberg ER, Juneja LR, Crocker PR, Varki N, Varki A. Loss of N-glycolylneuraminic acid in human evolution. Implications for sialic acid recognition by siglecs. J Biol Chem. 2000; 275:8633–8640. [PubMed: 10722703]
5. Tangvoranuntakul P, Gagneux P, Diaz S, Bardor M, Varki N, Varki A, Muchmore E. Human uptake and incorporation of an immunogenic nonhuman dietary sialic acid. Proc Natl Acad Sci USA. 2003; 100:12045–12050. [PubMed: 14523234]
6. Varki A. Colloquium paper: uniquely human evolution of sialic acid genetics and biology. Proc Natl Acad Sci USA. 2010; 107(Suppl 2):8939–8946. [PubMed: 20445087]
7. Varki NM, Strobert E, Dick EJ, Benirschke K, Varki A. Biomedical differences between human and nonhuman hominids: potential roles for uniquely human aspects of sialic acid biology. Annu Rev Pathol. 2011; 6:365–393. [PubMed: 21073341]
8. Crocker PR, Paulson JC, Varki A. Siglecs and their roles in the immune system. Nat Rev Immunol. 2007; 7:255–266. [PubMed: 17380156]
9. Varki A, Crocker PR. I-type Lectins. Essentials of Glycobiology. 2009
10. Ravetch JV, Lanier LL. Immune inhibitory receptors. Science. 2000; 290:84–89. [PubMed: 11021804]
11. Collins BE, Blixt O, DeSieno AR, Bovin N, Marth JD, Paulson JC. Masking of CD22 by cis ligands does not prevent redistribution of CD22 to sites of cell contact. Proc Natl Acad Sci USA. 2004; 101:6104–6109. [PubMed: 15079087]
12. Doody G, Justement L, Delibrias C, Matthews R, Lin J, Thomas M, Fearon D. A role in B cell activation for CD22 and the protein tyrosine phosphatase SHP. Science. 1995; 269:242–244. [PubMed: 7618087]
13. Taylor VC, Buckley CD, Douglas M, Cody AJ, Simmons DL, Freeman SD. The myeloid-specific sialic acid-binding receptor, CD33, associates with the protein-tyrosine phosphatases, SHP-1 and SHP-2. J Biol Chem. 1999; 274:11505–11512. [PubMed: 10206955]
14. Vitale C, Romagnani C, Falco M, Ponte M, Vitale M, Moretta A, Bacigalupo A, Moretta L, Mingari MC. Engagement of p75/AIRM1 or CD33 inhibits the proliferation of normal or leukemic myeloid cells. Proc Natl Acad Sci USA. 1999; 96:15091–15096. [PubMed: 10611343]
15. Ikehara Y, Ikehara SK, Paulson JC. Negative regulation of T cell receptor signaling by Siglec-7 (p70/AIRM) and Siglec-9. J Biol Chem. 2004; 279:43117–43125. [PubMed: 15292262]

16. Hoffmann A, Kerr S, Jellusova J, Zhang J, Weisel F, Wellmann U, Winkler TH, Kneitz B, Crocker PR, Nitschke L. Siglec-G is a B1 cell-inhibitory receptor that controls expansion and calcium signaling of the B1 cell population. Nat Immunol. 2007; 8:695–704. [PubMed: 17572677]

17. Yu Z, Maoui M, Wu L, Banville D, Shen S. mSiglec-E, a novel mouse CD33-related siglec (sialic acid-binding immunoglobulin-like lectin) that recruits Src homology 2 (SH2)-domain-containing protein tyrosine phosphatases SHP-1 and SHP-2. Biochem J. 2001; 353:483–492. [PubMed: 11171044]

18. Zhang M, Angata T, Cho JY, Miller M, Broide DH, Varki A. Defining the in vivo function of Siglec-F, a CD33-related Siglec expressed on mouse eosinophils. Blood. 2007; 109:4280–4287. [PubMed: 17272508]

19. Nguyen DH, Hurtado-Ziola N, Gagneux P, Varki A. Loss of Siglec expression on T lymphocytes during human evolution. Proc Natl Acad Sci USA. 2006; 103:7765–7770. [PubMed: 16682635]

20. Soto PC, Stein LL, Hurtado-Ziola N, Hedrick SM, Varki A. Relative over-reactivity of human versus chimpanzee lymphocytes: implications for the human diseases associated with immune activation. J Immunol. 2010; 184:4185–4195. [PubMed: 20231688]

21. Manno CS, Pierce GF, Arruda VR, Glader B, Ragni M, Rasko JJ, Rasko J, Ozelo MC, Hoots K, Blatt P, Konkle B, Dake M, Kaye R, Razavi M, Zajko A, Zehnder J, Rustagi PK, Nakai H, Chew A, Leonard D, Wright JF, Lessard RR, Sommer JM, Tigges M, Sabatino D, Luk A, Jiang H, Mingozzi F, Couto L, Ertl HC, High KA, Kay MA. Successful transduction of liver in hemophilia by AAV-Factor IX and limitations imposed by the host immune response. Nat Med. 2006; 12:342–347. [PubMed: 16474400]

22. Nathwani AC, Tuddenham EGD, Rangarajan S, Rosales C, McIntosh J, Linch DC, Chowdary P, Riddell A, Pie AJ, Harrington C, O'Beirne J, Smith K, Pasi J, Glader B, Rustagi P, Ng CYC, Kay MA, Zhou J, Spence Y, Morton CL, Allay J, Coleman J, Sleep S, Cunningham JM, Srivastava D, Basner-Tschakarjan E, Mingozzi F, High KA, Gray JT, Reiss UM, Nienhuis AW, Davidoff AM. Adenovirus-associated virus vector-mediated gene transfer in hemophilia B. N Engl J Med. 2011; 365:2357–2365. [PubMed: 22149959]

23. Mingozzi F, Maus MV, Hui DJ, Sabatino DE, Murphy SL, Rasko JEJ, Ragni MV, Manno CS, Sommer J, Jiang H, Pierce GF, Ertl HCJ, High KA. CD8(+) T-cell responses to adeno-associated virus capsid in humans. Nat Med. 2007; 13:419–422. [PubMed: 17369837]

24. Li H, Murphy SL, Giles-Davis W, Edmonson S, Xiang Z, Li Y, Lasaro MO, High KA, Ertl HC. Pre-existing AAV capsid-specific CD8+ T cells are unable to eliminate AAV-transduced hepatocytes. Mol Ther. 2007; 15:792–800. [PubMed: 17245353]

25. Wang L, Figueredo J, Calcedo R, Lin J, Wilson JM. Cross-presentation of adeno-associated virus serotype 2 capsids activates cytotoxic T cells but does not render hepatocytes effective cytolytic targets. Human Gene Therapy. 2007; 18:185–194. [PubMed: 17324107]

26. Li C, Hirsch M, DiPrimio N, Asokan A, Goudy K, Tisch R, Samulski RJ. Cytotoxic-T-lymphocyte-mediated elimination of target cells transduced with engineered adeno-associated virus type 2 vector in vivo. Journal of Virology. 2009; 83:6817–6824. [PubMed: 19369348]

27. Hedlund M, Tangvoranuntakul P, Takematsu H, Long JM, Housley GD, Kozutsumi Y, Suzuki A, Wynshaw-Boris A, Ryan AF, Gallo RL, Varki N, Varki A. N-glycolylneuraminic acid deficiency in mice: implications for human biology and evolution. Molecular and Cellular Biology. 2007; 27:4340–4346. [PubMed: 17420276]

28. Naito Y, Takematsu H, Koyama S, Miyake S, Yamamoto H, Fujinawa R, Sugai M, Okuno Y, Tsujimoto G, Yamaji T, Hashimoto Y, Itohara S, Kawasaki T, Suzuki A, Kozutsumi Y. Germinal center marker GL7 probes activation-dependent repression of N-glycolylneuraminic acid, a sialic acid species involved in the negative modulation of B-cell activation. Molecular and Cellular Biology. 2007; 27:3008–3022. [PubMed: 17296732]

29. Chandrasekharan K, Yoon JH, Xu Y, deVries S, Camboni M, Janssen PML, Varki A, Martin PT. A Human-Specific Deletion in Mouse Cmah Increases Disease Severity in the mdx Model of Duchenne Muscular Dystrophy. Science Translational Medicine. 2010; 2:42ra54 1–17.

30. Redelinghuys P, Antonopoulos A, Liu Y, Campanero-Rhodes MA, McKenzie E, Haslam SM, Dell A, Feizi T, Crocker PR. Early Murine T-lymphocyte Activation Is Accompanied by a Switch from N-Glycolyl- to N-Acetyl-neuraminic Acid and Generation of Ligands for Siglec-E. Journal of Biological Chemistry. 2011; 286:34522–34532. [PubMed: 21835922]

31. Pearce OMT, Varki A. Chemo-enzymatic synthesis of the carbohydrate antigen N-glycolylneuraminic acid from glucose. Carbohydr Res. 2010; 345:1225–1229. [PubMed: 20452577]
32. Sabatino D, Mingozzi F, Hui D, Chen H, Colosi P, Ertl HCJ, High KA. Identification of mouse AAV capsid-specific CD8+ T cell epitopes. Molecular Therapy. 2005; 12:1023–1033. [PubMed: 16263332]
33. Ahmed R, Salmi A, Butler LD, Chiller JM, Oldstone MB. Selection of genetic variants of lymphocytic choriomeningitis virus in spleens of persistently infected mice. Role in suppression of cytotoxic T lymphocyte response and viral persistence. J Exp Med. 1984; 160:521–540. [PubMed: 6332167]
34. Bardor M, Nguyen DH, Diaz S, Varki A. Mechanism of uptake and incorporation of the non-human sialic acid N-glycolylneuraminic acid into human cells. J Biol Chem. 2005; 280:4228–4237. [PubMed: 15557321]
35. Varki A, Gagneux P. Human-specific evolution of sialic acid targets: explaining the malignant malaria mystery? Proc Natl Acad Sci USA. 2009; 106:14739–14740. [PubMed: 19717444]
36. Sathish JG, Walters J, Luo JC, Johnson KG, Leroy FG, Brennan P, Kim KP, Gygi SP, Neel BG, Matthews RJ. CD22 is a functional ligand for SH2 domain-containing protein-tyrosine phosphatase-1 in primary T cells. J Biol Chem. 2004; 279:47783–47791. [PubMed: 15364920]
37. Sarkar S, Kalia V, Haining WN, Konieczny BT, Subramaniam S, Ahmed R. Functional and genomic profiling of effector CD8 T cell subsets with distinct memory fates. Journal of Experimental Medicine. 2008; 205:625–640. [PubMed: 18316415]
38. Jung YW, Rutishauser RL, Joshi NS, Haberman AM, Kaech SM. Differential localization of effector and memory CD8 T cell subsets in lymphoid organs during acute viral infection. J Immunol. 2010; 185:5315–5325. [PubMed: 20921525]
39. Kaech SM, Wherry EJ. Heterogeneity and cell-fate decisions in effector and memory CD8+ T cell differentiation during viral infection. Immunity. 2007; 27:393–405. [PubMed: 17892848]
40. Wherry EJ, Ahmed R. Memory CD8 T-cell differentiation during viral infection. Journal of Virology. 2004; 78:5535–5545. [PubMed: 15140950]
41. Jameson SC, Masopust D. Diversity in T cell memory: an embarrassment of riches. Immunity. 2009; 31:859–871. [PubMed: 20064446]
42. Sarkar S, Teichgräber V, Kalia V, Polley A, Masopust D, Harrington LE, Ahmed R, Wherry EJ. Strength of stimulus and clonal competition impact the rate of memory CD8 T cell differentiation. J Immunol. 2007; 179:6704–6714. [PubMed: 17982060]
43. Li H, Lin SW, Giles-Davis W, Li Y, Zhou D, Xiang ZQ, High KA, Ertl HCJ. A preclinical animal model to assess the effect of pre-existing immunity on AAV-mediated gene transfer. Mol Ther. 2009; 17:1215–1224. [PubMed: 19367258]
44. Mingozzi F, High KA. Therapeutic in vivo gene transfer for genetic disease using AAV: progress and challenges. Nat Rev Genet. 2011; 12:341–355. [PubMed: 21499295]
45. Li H, Lasaro MO, Jia B, Lin SW, Haut LH, High KA, Ertl HCJ. Capsid-specific T-cell Responses to Natural Infections With Adeno-associated Viruses in Humans Differ From Those of Nonhuman Primates. Mol Ther. 2011; 19:2021–2030. [PubMed: 21587208]
46. Mingozzi F, Hasbrouck NC, Basner-Tschakarjan E, Edmonson SA, Hui DJ, Sabatino DE, Zhou S, Wright JF, Jiang H, Pierce GF, Arruda VR, High KA. Modulation of tolerance to the transgene product in a nonhuman primate model of AAV-mediated gene transfer to liver. Blood. 2007; 110:2334–2341. [PubMed: 17609423]
47. Nathwani AC, Gray JT, McIntosh J, Ng CYC, Zhou J, Spence Y, Cochrane M, Gray E, Tuddenham EGD, Davidoff AM. Safe and efficient transduction of the liver after peripheral vein infusion of self-complementary AAV vector results in stable therapeutic expression of human FIX in nonhuman primates. Blood. 2007; 109:1414–1421. [PubMed: 17090654]
48. Nathwani AC, Rosales C, McIntosh J, Rastegarlari G, Nathwani D, Raj D, Nawathe S, Waddington SN, Bronson R, Jackson S, Donahue RE, High KA, Mingozzi F, Ng CYC, Zhou J, Spence Y, McCarville MB, Valentine M, Allay J, Coleman J, Sleep S, Gray JT, Nienhuis AW, Davidoff AM. Long-term safety and efficacy following systemic administration of a self-

complementary AAV vector encoding human FIX pseudotyped with serotype 5 and 8 capsid proteins. Mol Ther. 2011; 19:876–885. [PubMed: 21245849]

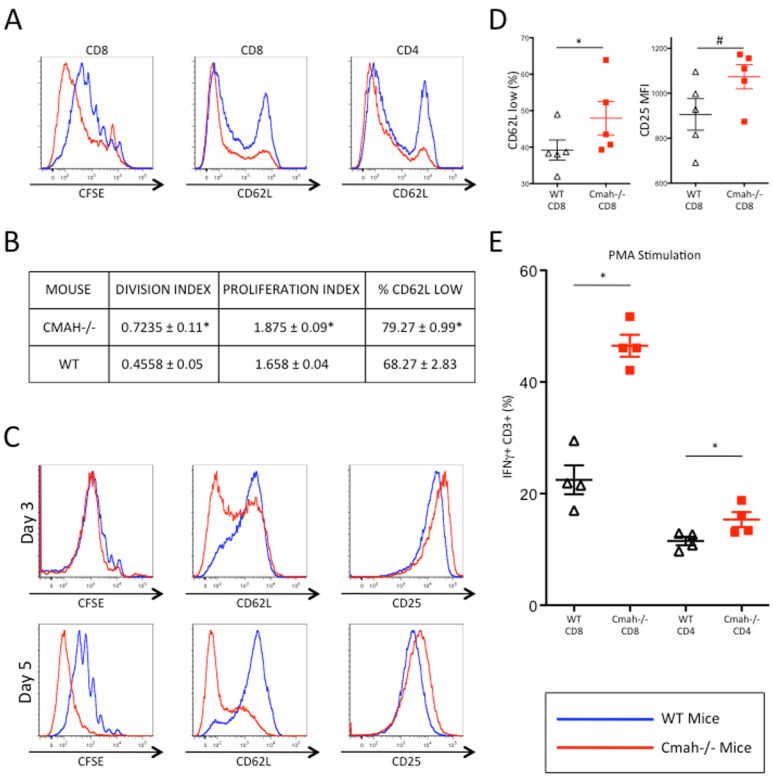

MOUSE	DIVISION INDEX	PROLIFERATION INDEX	% CD62L LOW
CMAH-/-	0.7235 ± 0.11*	1.875 ± 0.09*	79.27 ± 0.99*
WT	0.4558 ± 0.05	1.658 ± 0.04	68.27 ± 2.83

Figure 1. In Vitro T Cell Proliferation and Activation is Augmented in Cmah−/− Mice

(A and C) CFSE-labeled mouse splenocytes (A) or negatively isolated CD8+ T cells (C) were activated in culture for 3 or 5 days with α-CD3 α-CD28 beads. Proliferation was assayed by visualizing CFSE dilution (left most panels), while CD62L and CD25 expression was used to quantify activation differences (middle and right panels). Red-shaded lines represent either representative Cmah−/− mice (A) or Cmah−/− isolated CD8+ T cells (C), while blue-shaded lines represent either representative WT mice (A) or WT isolated CD8+ T cells (C). (B) CFSE-labeled mouse splenocytes were activated in culture for 5 days with α-CD3 α-CD28 beads. Proliferation indices and division indices on CD8 T cells were calculated based on analysis of CFSE dilution. (D) Mouse splenocytes were activated in culture for 5 hours with α-CD3 α-CD28 beads, and assayed for CD62L (left panel) and CD25 (right panel). (E) Mouse splenocytes were stimulated with PMA for 5 hours and assayed for IFNγ production. Black triangles – WT cells, red squares Cmah−/− cells. *p 0.05, #p<0.1, student's t test. N=5 mice per group (A, B, D), pooled T cells isolated from 5 mice per group (C), and 4 mice per group (E). Results are representative of at least two experiments.

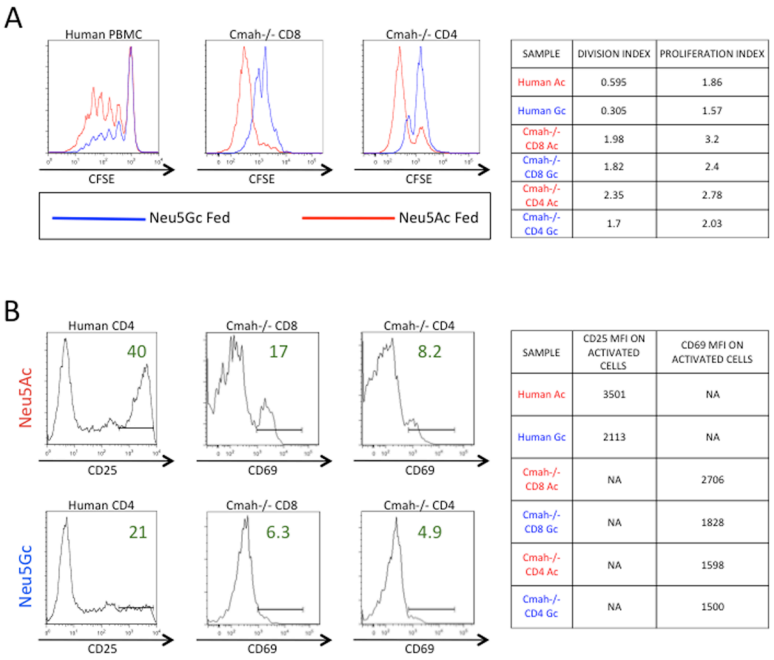

SAMPLE	DIVISION INDEX	PROLIFERATION INDEX
Human Ac	0.595	1.86
Human Gc	0.305	1.57
Cmah-/- CD8 Ac	1.98	3.2
Cmah-/- CD8 Gc	1.82	2.4
Cmah-/- CD4 Ac	2.35	2.78
Cmah-/- CD4 Gc	1.7	2.03

SAMPLE	CD25 MFI ON ACTIVATED CELLS	CD69 MFI ON ACTIVATED CELLS
Human Ac	3501	NA
Human Gc	2113	NA
Cmah-/- CD8 Ac	NA	2706
Cmah-/- CD8 Gc	NA	1828
Cmah-/- CD4 Ac	NA	1598
Cmah-/- CD4 Gc	NA	1500

Figure 2. Metabolically re-introducing Neu5Gc to Cmah−/− T Cells and Human T Cells Blunts Proliferation and Activation

(A) CFSE-labeled Human PBMC (left panel) or Cmah−/− mouse T cells pooled from 5 mice (middle and right panels) were stimulated with immobilized α-CD3 and soluble α-CD28 for 5 days in either Neu5Gc-containing media (blue line) or Neu5Ac-containing control media (red line), then collected and assayed for proliferation via CFSE dilution. Table on right summarizes the proliferation and division indices from these experiments. (B) Human CD4 T cells were pre-incubated in Neu5Gc or Neu5Ac media for 3 days, activated for two days as above, and then assayed for activation via CD25 expression. Cmah−/− T cells were pre-incubated in Neu5Gc or Neu5Ac media for 2 days, activated for 5 days as above, and then assayed for activation via CD69 expression. Table on right summarizes the mean fluorescent intensity of the assayed activation markers on positively expressing cells. Results are representative of at least three experiments on either pooled Cmah−/− mouse T cells (5 mice) or individual human donors.

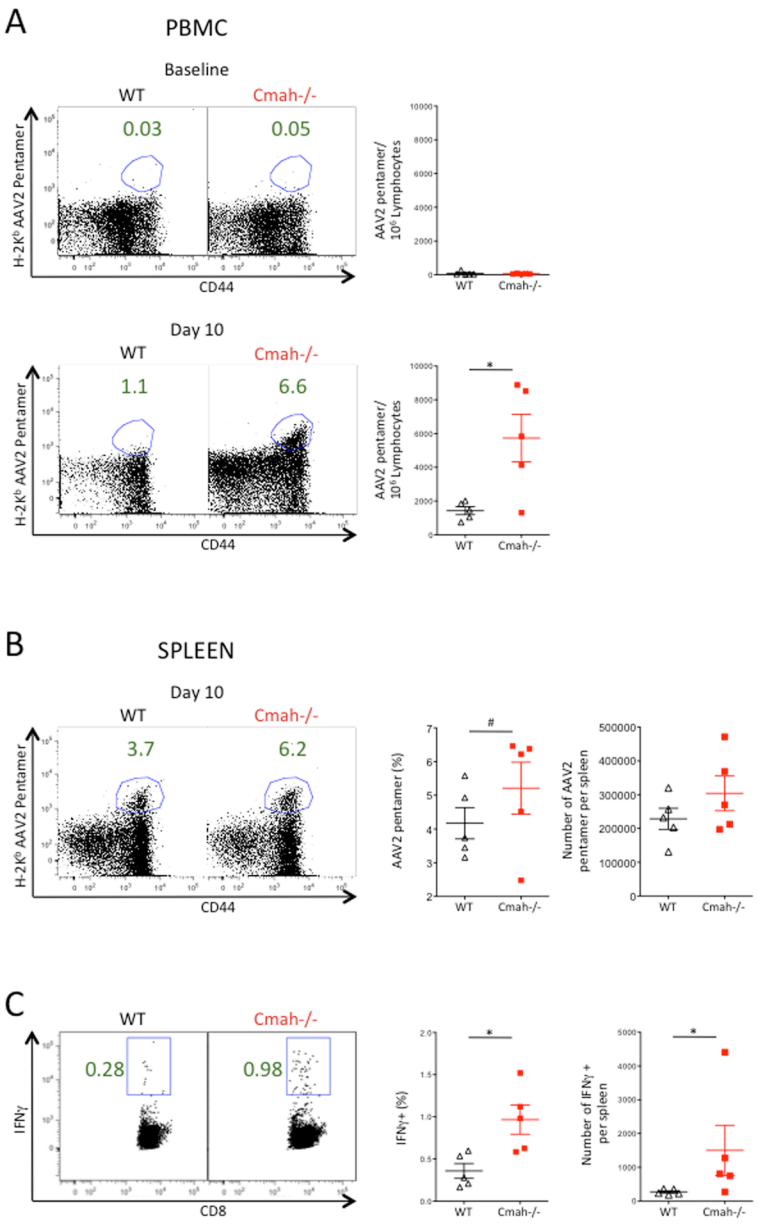

Figure 3. Cmah−/− Mice Mount a Greater CD8 T Cell Response to AAV after Ad-AAV Immunization

Mice were immunized with human Adenovirus serotype 5 intramuscularly. (A) Representative frequency of H-2K^b AAV2-Pentamer+ CD8+ T cells in the blood at baseline (top) and day 10 (bottom) of WT (left panels) and Cmah−/− (middle panels) mice and the number of H-2K^b AAV2-Pentamer+ CD8+ T cells per IE6 lymphocytes (right panels). (B) Representative frequency of H-2K^b AAV2-Pentamer+ CD8+ T cells in the spleen at day 10 of WT (left panel) and Cmah−/− (middle left panel) mice and the frequency of H-2K^b AAV2-Pentamer+ CD8+ T cells (middle right panel). Absolute numbers of H-2K^b AAV2-Pentamer+ CD8+ T cells is plotted in the far right panel. (C) Representative Frequency of IFNγ+ CD8 T Cells in day 10 spleens of WT (left panel) and Cmah−/− (middle left panel) mice after 5 hours of H-2K^b AAV2 peptide SNYNKSVNV stimulation, and the summary plot of all frequencies in each group (middle right panel). Absolute numbers of IFNγ+ CD8

T cells is plotted in the far right panel. *p<0.05, #p<0.1, student's t test. N=5 mice per group. Results are representative of at least two experiments.

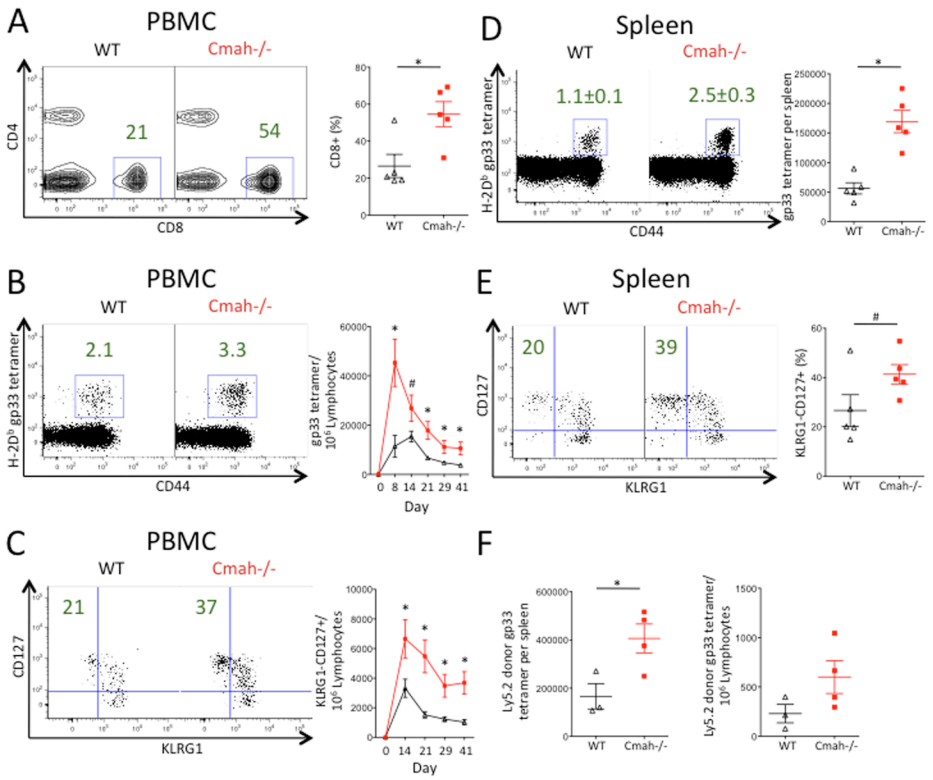

Figure 4. Cmah−/− Mice Mount a Greater T Cell Response During Acute LCMV Armstrong Infection

Mice were infected with acute LCMV strain Armstrong and bled at various time points until sacrifice and spleen isolation at day 42. (A–C) Mouse PBMC. (A) Frequency of CD8+ T cells at day 8 in the blood of WT (left plot and black triangles in right plot) and Cmah−/− (middle plot and red squares in right plot) mice. Left and middle plots show the median representative dot plots from each group, while the plot on the right shows quantification of the frequencies. (B) Number of LCMV H2-D^b gp33 tetramer+ CD8+ T cells per 1E6 lymphocytes in the blood of WT (black line, right plot) and Cmah−/− (red line, right plot) mice over 42 days. Left and middle plots show the median representative dot plots from day 42 from each group, while the right plot graphs the number of tetramer+ cells per 1E6 lymphocytes over time. (C) Number of LCMV H2-D^b gp33 tetramer+ CD8+ T cells that are KLRG1-CD127+ per 1E6 lymphocytes in the blood of WT (black line, right plot) and Cmah −/− (red line, right plot) mice over 42 days. Left and middle plots show the median representative dot plots from day 42 from each group, while the right plot graphs the number of memory-phenotype tetramer+ cells per 1E6 lymphocytes over time. (D and E) Mouse splenocytes at day 42. (D) Left and middle plots show the median representative dot plots of the frequencies of LCMV H2-D^b gp33 tetramer+ CD8+ splenocytes from day 42 from each group, while the plot on the right shows quantification of the absolute numbers of these cells in the spleen. WT (black triangles in right plot) and Cmah−/− (red squares in right plot). Similar trends were observed in the number of gp276 tetramer+ CD8+ splenocytes. (E) Left and middle plots show the median representative dot plots of the frequencies of KLRG1-CD127+ LCMV H2-D^b gp33 tetramer+ CD8+ splenocytes, while the plot on the right shows quantification of these frequencies in WT (black triangles in right plot) and Cmah−/− (red squares in right plot) spleens. (F) Day 7 CD8 donor (Ly5.2) analysis in Ly5.1 recipient mice infected with LCMV. Left plot shows the number of gp33+ CD8+ donor T cells per spleen, and right plot shows the number of gp33+ CD8+ donor T cells per 1E6 lymphocytes in the

blood. Cmah−/− (red squares, 4 mice), WT (black triangles, 3 mice). *$p<0.05$, #$p<0.1$, student's t test. N=5 mice per group (A–E). Results are representative of at least two experiments.

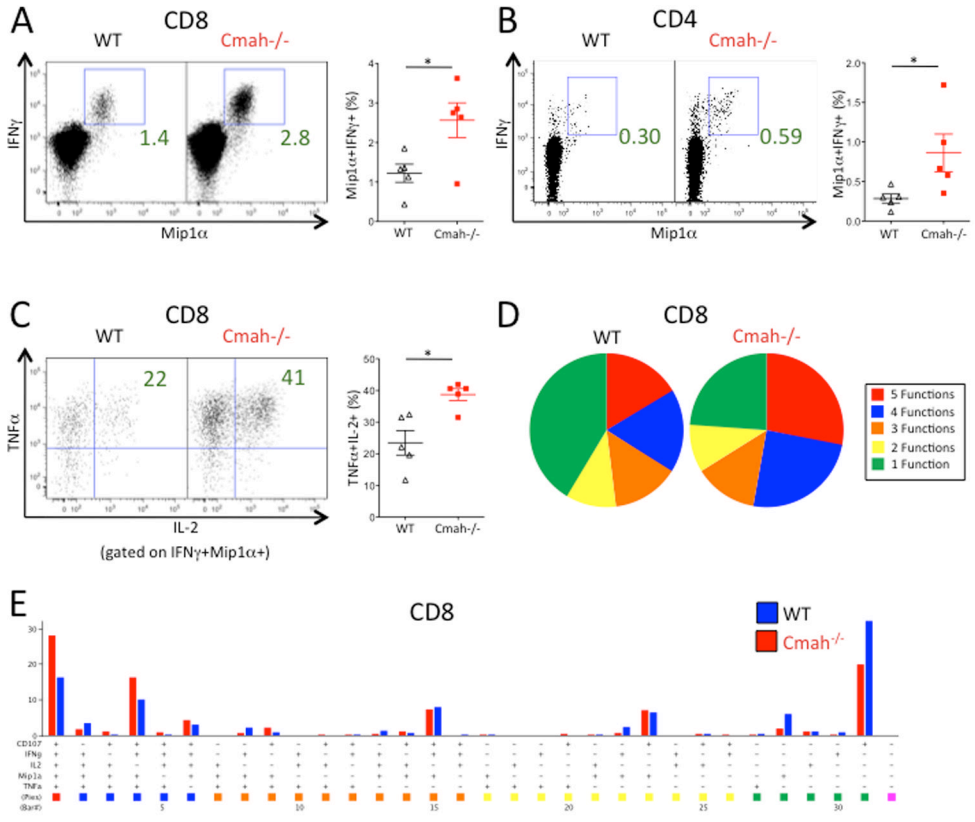

Figure 5. LCMV-specific T Cells in Cmah−/− Mice Produce a Higher Proportion of Cytokines Than WT T Cells

Mice infected with acute LCMV Armstrong were sacrificed at day 42, and isolated splenocytes were stimulated for 5 hours with LCMV peptides and stained for multiple cytokines to assay functionality. (A, C–E) Functionality of CD8+ T cells upon LCMV peptide GP276 stimulation. (A) Frequency of Mip1α+IFNγ+ CD8+ T cells upon LCMV peptide stimulation in WT (black triangles in right plot) and Cmah−/− (red squares in right plot) mice. Left and middle plots show the median representative dot plots from each group, while the right plot shows the quantification of the frequencies. (B) Frequency of Mip1α +IFNγ+ CD4+ T cells upon LCMV peptide GP66-77 stimulation in WT (black triangles in right plot) and Cmah−/− (red squares in right plot) mice. Left and middle plots show the median representative dot plots from each group, while the right plot shows the quantification of the frequencies. (C) Frequency of Mip1α+IFNγ+ CD8+ T cells from (A) that are TNFα+IL-2+. Representative plots on the left and middle, quantification on the right as described in (A). (D) Polyfunctional pie charts of day 42 stimulated CD8+ T cells from WT (left pie chart) and Cmah−/− (right pie chart) mice. Red=5 functions, blue=4 functions, orange=3 functions, yellow=2 functions, green=one function. Functions= CD107a, Mip1α, IFNγ, TNFα, and IL-2. (E) Bar graph representation of each combination of the functions defined in (D) between WT (blue bars) and Cmah−/− (red bars) CD8+ T cells, with the corresponding pie chart color on the bottom. *p<0.05, student's t test. N=5 mice per group. Results are representative of at least two experiments.